

# Zero-shot Commonsense Reasoning over Machine Imagination

Anonymous ACL submission

## Abstract

Recent approaches to zero-shot commonsense reasoning have enabled Pre-trained Language Models (PLMs) to learn a broad range of commonsense knowledge without being tailored to specific situations. However, they often suffer from human reporting bias inherent in textual commonsense knowledge, leading to discrepancies in understanding between PLMs and humans. In this work, we aim to bridge this gap by introducing an additional information channel to PLMs. We propose IMAGINE (Machine **I**magination-based **R**easoning), a novel zero-shot commonsense reasoning framework designed to complement textual inputs with visual signals derived from machine-generated images. To achieve this, we enhance PLMs with imagination capabilities by incorporating an image generator into the reasoning process. To guide PLMs in effectively leveraging machine imagination, we create a synthetic pre-training dataset that simulates visual question-answering. Our extensive experiments on diverse reasoning benchmarks and analysis show that IMAGINE outperforms existing methods by a large margin, highlighting the strength of machine imagination in mitigating reporting bias and enhancing generalization capabilities<sup>1</sup>.

## 1 Introduction

Commonsense reasoning has been considered a crucial milestone in the pursuit of artificial general intelligence (Gunning, 2018). While Pre-trained Language Models (PLMs; Devlin et al., 2019; Brown et al., 2020) often exhibit near-human reasoning capabilities after being fine-tuned on specific commonsense datasets, they face challenges in zero-shot scenarios where examples differ significantly from their training data distribution (Mitra et al., 2019; Kim et al., 2022). Overcoming this limitation

<sup>1</sup>Our code and data are available at <https://anonymous4open.science/r/Imagine-C35A>

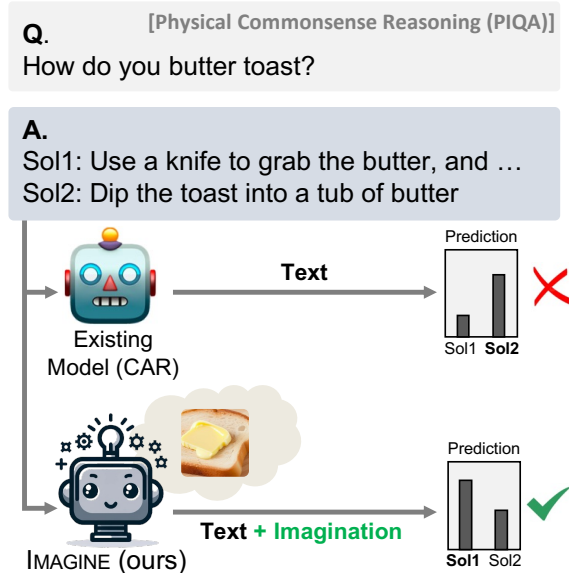


Figure 1: Example from the PIQA (Bisk et al., 2020) with model predictions. Compared to the existing methods, IMAGINE performs reasoning with imagination.

is crucial for achieving human-level proficiency in natural language understanding.

One promising approach to this limitation is injecting commonsense knowledge from external Knowledge Bases (KBs; Sap et al., 2019a; He et al., 2022b) into PLMs. Specifically, this involves transforming knowledge entities into a question-answering (QA) format, resulting in a synthetic QA dataset. This constructed dataset is then used to train PLMs similarly to the pre-training phase. Since the knowledge bases can cover a wide spectrum of commonsense knowledge, this approach leads to substantial improvements in reasoning ability across diverse situations without specializing in specific knowledge (Wang et al., 2023, 2024).

However, they often suffer from human reporting bias (Gordon and Durme, 2013), as textual commonsense knowledge only captures the most frequently occurring scenarios, thereby neglecting

058 less common but equally critical knowledge nec-  
059 essary for comprehensive reasoning. Figure 1 il-  
060 lustrates a case where a recent model (Wang et al.,  
061 2023) fails to accurately reason about the question  
062 “*How do you butter toast?*”. Since the existing mod-  
063 els rely solely on textual inputs, they often neglect  
064 contextual details, such as the fact that butter is typ-  
065 ically too solid to be dipped. In contrast, humans  
066 can easily answer such questions by visually imag-  
067 ining the shape, solidity, and interactions of butter  
068 with other objects. This observation motivates us  
069 to explore additional modalities to complement tex-  
070 tual commonsense knowledge.

071 In this paper, we introduce IMAGINE (Machine  
072 **I**magination-based Reasoning), a novel zero-shot  
073 commonsense reasoning framework designed to  
074 circumvent the reporting bias inherent in textual  
075 inputs. Inspired by the cognitive studies highlight-  
076 ing the beneficial effects of visual imagery on lan-  
077 guage understanding (Gambrell and Bales, 1986;  
078 Dessalegn and Landau, 2013), IMAGINE is de-  
079 signed to leverage visual signals to complement tex-  
080 tual inputs. To achieve this, we integrate PLMs with  
081 a conditional image generator, enabling machine  
082 imagination capabilities. To guide the model in  
083 learning to utilize visual and textual inputs jointly,  
084 we create a synthetic VQA dataset, which is then  
085 used to optimize PLMs. By acquiring a broad spec-  
086 trum of commonsense knowledge along with visual  
087 signals, IMAGINE enhances reasoning capabilities  
088 while circumventing human reporting bias.

089 To verify the effectiveness of IMAGINE, we per-  
090 form extensive experiments, encompassing diverse  
091 reasoning benchmarks, architectures, and scales.  
092 The experimental results convincingly demonstrate  
093 that IMAGINE surpasses existing methods, includ-  
094 ing large language models, in reasoning capabili-  
095 ties. Moreover, our in-depth analysis reveals that  
096 IMAGINE effectively enables PLMs to adaptively  
097 leverage machine imagination capabilities in a ben-  
098 eficial manner. The contributions of this paper in-  
099 clude the following:

- We introduce IMAGINE, a novel zero-shot commonsense reasoning framework, aimed at mitigating reporting bias and enhancing the generalizability of PLMs.
- We construct a synthetic VQA dataset to enable PLMs to jointly utilize textual and visual signals while achieving commonsense reasoning ability.

- We demonstrate that IMAGINE surpasses state-of-the-art zero-shot reasoning models across diverse reasoning tasks, highlighting the significance of machine imagination.

## 2 Related Work

### 2.1 Zero-shot Commonsense Reasoning

There are two major approaches to zero-shot commonsense reasoning. The first approach involves utilizing the inherent capabilities of the off-the-shelf PLMs without updating their parameters. For example, Trinh and Le (2018) utilized the perplexity of vanilla language modeling, and Li et al. (2022) leveraged PLMs with specifically-designed prompting. Shwartz et al. (2020) solicited the commonsense knowledge from the language models through an iterative self-talk. Similarly, Dou and Peng (2022) obtained additional knowledge for reasoning based on the cloze-style translation. The second approach involves leveraging external commonsense knowledge bases (e.g., ATOMIC (Sap et al., 2019a), ConceptNet (Speer et al., 2017)) to provide language models with additional knowledge. Specifically, recent studies have transformed the knowledge entities (e.g., triplets of (head, relation, tail)) into synthetic QA pairs and trained the models with them (Banerjee and Baral, 2020; Ma et al., 2021). Recently, Wang et al. (2023) further improved the synthetic signals through a conceptualization process (Song et al., 2011) which abstracts a commonsense knowledge triplet to many higher-level instances. Subsequently, Wang et al. (2024) injected the instantiation phase into the process of synthetic dataset generation with the help of the generation capabilities of LLMs.

### 2.2 Visual Information for Natural Language Understanding

A few previous works have leveraged machine imagination to address Natural Language Understanding (NLU) problems. For example, Tan and Bansal (2020) proposed VOKEN, which introduces visual supervision into language model pre-training by incorporating external knowledge from images retrieved for the tokens. Instead of retrieving visual information, Lu et al. (2022) proposed generating synthetic images (i.e., imagination) based on a generative model to tackle downstream NLU tasks. In the context of commonsense reasoning, Liu et al. (2022) utilized visual information to comprehend spatial commonsense knowledge (e.g., *how big is a*

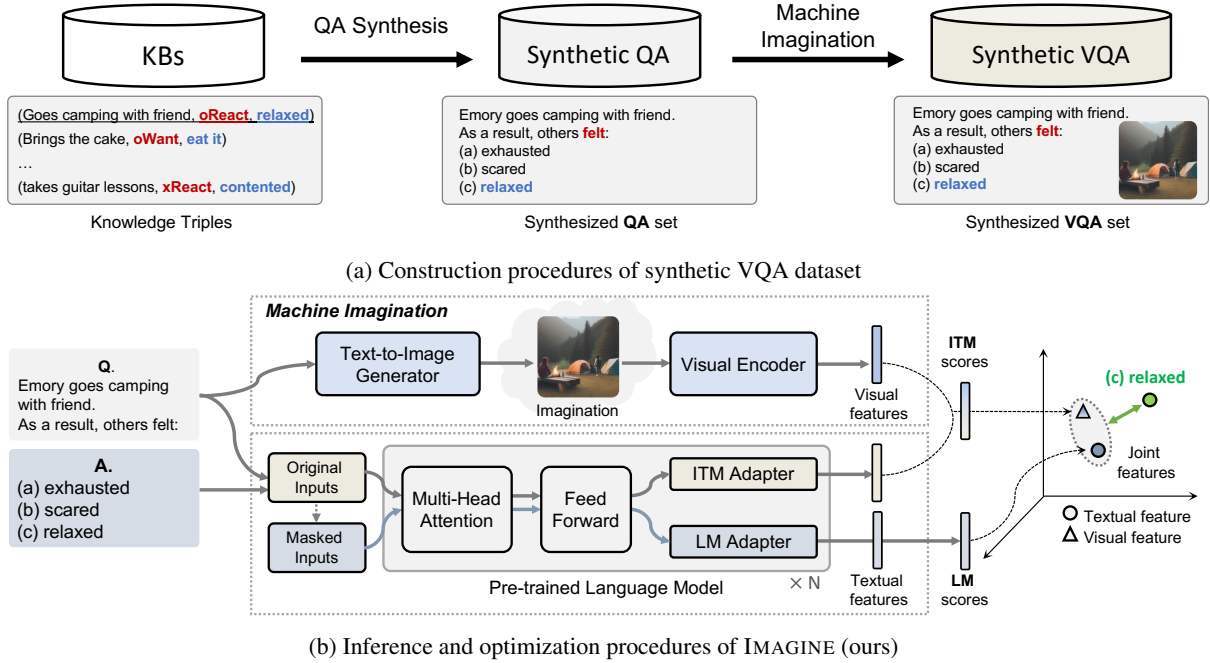


Figure 2: Overall procedures for (a) constructing a synthetic VQA dataset and (b) the inference/optimization phase of IMAGINE (ours) using the given QA pair. The process starts with the textual pair consisting of a question and its answers, followed by the generation of visual signals (i.e., imagination) conditioned on the question. The two distinct features from visual and textual models are then utilized to derive a comprehensive prediction.

lion?). Similar to the proposed method, Yang et al. (2022) introduced Z-LaVI, which integrated visual information with PLMs through both retrieval and synthesis to achieve zero-shot reasoning abilities.

**3 Machine Imagination-based Reasoning**

In this section, we elaborate on the proposed method, namely IMAGINE (Machine **Imagination**-based Reasoning), for zero-shot commonsense reasoning. The core strategy is to complement textual commonsense knowledge with visual signals derived from machine-generated images. To achieve this, we first couple the PLMs with a text-to-image generator (§3.1), enabling machine imagination in text-based PLMs. We then construct a large-scale synthetic VQA dataset to learn the joint use of textual and visual signals in the reasoning process (§3.2). By optimizing the model with additional signals that encapsulate commonsense knowledge, IMAGINE can effectively perform commonsense reasoning while avoiding human reporting bias inherent in textual inputs (§3.3, §3.4). The overall procedure is depicted in Figure 2.

### 3.1 Machine Imagination in PLMs

We start by introducing the machine imagination in text-based PLMs. We denote PLMs as  $\mathcal{M}_T$ , which

serve as the backbone for zero-shot commonsense reasoning. For machine imagination, we incorporate two additional models to process visual signals. Specifically, we introduce: (i) a text-to-image generator,  $\mathcal{M}_{T2I}$ , which creates relevant images by conditioning the textual inputs, and (ii) a visual encoder,  $\mathcal{M}_I$ , which acts as a feature extractor for the given images.

The overall mechanism of machine imagination operates as follows: Given a textual input, the text-to-image model  $\mathcal{M}_{T2I}$  initially generates an image that captures the essence of the text. With these generated images linked to textual inputs, both PLMs,  $\mathcal{M}_T$ , and the visual encoder,  $\mathcal{M}_I$ , jointly encode the textual input and the generated image. The resultant features are then utilized to derive the comprehensive predictions.

### 3.2 Synthetic VQA Construction

Following the previous works (Ma et al., 2021; Wang et al., 2023), we achieve zero-shot commonsense reasoning ability by constructing the synthetic QA dataset from the knowledge base. On top of this dataset, we build a synthetic visual question-answering (synthetic VQA) dataset with the help of machine imagination. The dataset is designed to: (i) instill commonsense reasoning abilities in

	<p>Q: Emory is walking home. Emory is seen as...</p> <p>A1: Bossy <b>A2: Tired</b> A3: Independent</p>		<p>Q: <u>A group of people walking down a street.</u> Where is this scene from?</p> <p>A1: This scene takes place in a university <b>A2: It looks like the middle east</b> A3: This scene is set before the nineteen hundreds</p>
	<p>Q: Berkeley folds his tent. Berkeley is seen as...</p> <p>A1: Withdrawn A2: Dedicated <b>A3: Adventurous</b></p>		<p>Q: <u>A man and a woman sitting at a bar.</u> Is Sam currently drunk?</p> <p>A1: Yes, Bali recently drank alcohol <b>A2: Yes, Sam is intoxicated</b> A3: Possibly, but not presently</p>

Figure 3: Examples of the Synthetic VQA dataset. The examples on the left are sourced from AbstractATOMIC (Wang et al., 2023), while the two examples on the right are sourced from VCR (Zellers et al., 2019). **Bold** indicates the correct answer, and underline denotes the generated image caption.

PLMs and (ii) teach them to harmoniously utilize both textual and visual inputs.

The objective of this process is to construct VQA pairs  $(Q, A, I)$ , where each pair includes a natural language question  $Q$ , a set of  $n$  answer choices  $A = A_1, A_2, \dots, A_n$ , including one ground-truth answer and  $n - 1$  distractors, along with an image  $I$  that corresponds to the question.

**Synthetic QA** We first construct textual QA pairs from the KBs by following the recent work (Wang et al., 2023). Specifically, we transform the knowledge entities into the QA pairs through the conceptualized augmentation of the entities (Wang et al., 2023) with the pre-defined natural language templates (e.g., the relation of *xWant* is transformed to *As a result, PersonX wanted to*). This process results in textual synthetic QA pairs  $(Q, A)$ .

**Synthetic VQA** On the textual synthetic QA pairs, we input the textual question  $Q$  to the text-to-image model  $\mathcal{M}_{T2I}$  to generate the visual counterpart  $I$  that depicts the scenarios described in each question. These generated images provide an additional layer of information, offering a visual context that enhances the reasoning ability based not only on textual descriptions but also on visual evidence. This augmentation leverages the strengths of visual imagery on language understanding (Gambrell and Bales, 1986; Dessalegn and Landau, 2013), potentially improving the robustness and accuracy of the model predictions.

However, relying solely on the synthetic relationships between QA pairs and generated images can introduce challenges related to the alignment of visual content since machines often fail to generate well-aligned images with textual inputs (Feng et al., 2023). Therefore, we augment the synthetic VQA pairs with the widely used Visual Commonsense

Reasoning (VCR) dataset (Zellers et al., 2019). Each pair from this dataset consists of  $(Q, A, R, I)$ , where  $R$  is a rationale for the correct answer; however, we omit  $R$  since our focus is on the QA pairs associated with relevant images. Additionally, to enrich the input and enhance visual comprehension for PLMs, we generate textual context information for each image using an image captioning model<sup>2</sup>, which we prepend as a prefix to each  $Q$ <sup>3</sup>.

### 3.3 Pre-training IMAGINE on Synthetic VQA

Based on the synthetic VQA dataset, we integrate commonsense knowledge into the models. Since IMAGINE involves two distinct modalities (i.e., text and image), we introduce two separate objectives to select the best answer choice: Language Modeling (LM) and Image-Text Matching (ITM). To obtain the LM scores, we calculate the masked language modeling loss for the Transformer encoder-based model, formulated as:

$$S_{LM}(T) = -\frac{1}{m} \sum_{t=1}^m \log P(w_t | \dots w_{t-1}, w_{t+1} \dots). \quad (1)$$

For the decoder-based model, we compute the autoregressive language modeling loss, defined as:

$$S_{LM}(T) = -\frac{1}{m} \sum_{t=1}^m \log P(w_t | w_1 \dots w_{t-1}), \quad (2)$$

where  $w_i$  denotes the  $i$ -th word, and  $m$  is the number of tokens in the sequence  $T$ . To compute the ITM scores, we first contextualize the visual features based on the textual sequences. Let the visual features from the visual encoder  $\mathcal{M}_I$  be denoted as

<sup>2</sup>We use InstructBLIP (Dai et al., 2023) for captioning.

<sup>3</sup>More details of synthetic VQA are in Appendix A.

273  $V$ , we derive the contextualized visual features as  
274 follows:

275 
$$C = \text{softmax}\left(\frac{\bar{T}V^\top}{\sqrt{d_v}}\right)V, \quad (3)$$

276 where  $\bar{T}$  is the feature vector from the PLMs  $\mathcal{M}_T$ .  
277 For the encoder-based model, we use the final hidden  
278 state of the [CLS] token as the context vector,  
279 and for the decoder-based model, we use the hidden  
280 state of the last token as the context vector.  $d_v$  is the  
281 dimension of visual features. We then achieve the  
282 ITM scores by calculating the similarity between  
283 contextualized visual features and textual features  
284 as follows:

285 
$$S_I(T, V) = \text{sim}(\vec{T}, C), \quad (4)$$

286 where  $\text{sim}(\cdot)$  denotes the cosine similarity function.  
287 By combining two different scores, we produce the  
288 joint scores  $S_J$  as follows:

289 
$$S_J(T, V) = \frac{1}{2}(S_M(T) + S_I(T, V)), \quad (5)$$

290 After calculating all scores  $S^{(1)}, S^{(2)}, \dots, S^{(n)}$  for  
291  $n$  answer candidates, we calculate the marginal  
292 ranking loss defined as:

293 
$$\mathcal{L}_{QA}(S) = \frac{1}{n} \sum_{i=1, i \neq y}^n \max(0, \eta - S^{(y)} + S^{(i)}), \quad (6)$$

294 where  $y$  indicates the index of the correct answer  
295 and  $\eta$  is the pre-defined margin. The overall objectives  
296 are as follows:

297 
$$\mathcal{L} = \mathcal{L}_{QA}(S_M) + \mathcal{L}_{QA}(S_I) + \mathcal{L}_{QA}(S_J). \quad (7)$$

298 However, we have empirically observed that the  
299 ITM objective prevents the model from learning  
300 the LM objective, which is essential for developing  
301 reasoning capabilities. To mitigate the conflict  
302 between these two objectives, we introduce two  
303 distinct adapters (He et al., 2022a), LM adapter  
304 and ITM adapter. Each adapter is trained separately  
305 with a different focus. It is important to note that  
306 only the weights within these adapters are opti-  
307 mized during training; all other parameters remain  
308 frozen. By separating the parameters for objectives,  
309 we can effectively reduce conflicts between them.

### 3.4 Inference from IMAGINE

311 For the zero-shot evaluation, we use the same strat-  
312 egy to compute the LM and ITM scores after syn-  
313 thesizing the image based on the question. How-  
314 ever, we ensemble two scores to derive the model’s

315 prediction after obtaining the probability distribu-  
316 tion through softmax.

317 
$$P(S) = \text{softmax}(S^{(1)}, S^{(2)}, \dots, S^{(n)}), \quad (8)$$

318 
$$P(A|Q) = (1 - \lambda) \cdot P(S_M) + \lambda \cdot P(S_I), \quad (9)$$

319 where  $\lambda$  is an ensemble coefficient that controls the  
320 contributions between textual and visual features.

## 4 Experiments

322 In this section, we demonstrate the effectiveness  
323 of IMAGINE. Specifically, we conduct extensive  
324 experiments and analysis to answer the following  
325 research questions:

326 **Q1 (Generalizability)** Does IMAGINE offer bet-  
327 ter zero-shot performance across a broad  
328 range of reasoning benchmarks? (§4.2)

329 **Q2 (Multimodality)** Does IMAGINE effectively  
330 integrate visual signals (imagination) with tex-  
331 tual knowledge? (§4.3, §4.4)

332 **Q3 (Effectiveness)** How effective are the compo-  
333 nents of IMAGINE in zero-shot commonsense  
334 reasoning? (§4.5)

### 4.1 Experimental Setup

336 **Dataset.** Following the previous works on zero-  
337 shot reasoning (Ma et al., 2021; Yang et al., 2022),  
338 we evaluate our framework on commonsense rea-  
339 soning tasks and science QA tasks to assess its gen-  
340 eralizability. Specifically, we evaluate each base-  
341 line on the five reasoning benchmarks, including  
342 Abductive NLI ( $\alpha$ NLI; Bhagavatula et al., 2020),  
343 CommonsenseQA (CSQA; Talmor et al., 2019),  
344 PhysicalIQA (PIQA; Bisk et al., 2020), SocialIQA  
345 (SIQA; Sap et al., 2019b), and Winogrande (WG;  
346 Sakaguchi et al., 2020). These datasets vary sig-  
347 nificantly in format (e.g., natural language infer-  
348 ence, QA, pronoun resolution) and required knowl-  
349 edge (e.g., social and physical knowledge for SIQA  
350 and PIQA, respectively), enabling a comprehen-  
351 sive evaluation of a wide spectrum of reasoning  
352 capabilities. For science QA tasks, we assess each  
353 baseline on the four benchmarks, including QA via  
354 Sentence Composition (QASC; Khot et al., 2020),  
355 Science Questions (SciQ; Welbl et al., 2017), and  
356 the AI2 Reasoning Challenge (ARC-Easy, ARC-  
357 Challenge; Clark et al., 2018). Given that science  
358 QA datasets often contain various types of report-  
359 ing bias, such as color and shape biases, we selected  
360 these datasets to verify the efficacy of IMAGINE in  
361 mitigating reporting bias.

Method	KB	$\alpha$ NLI	CSQA	PIQA	SIQA	WG	Avg.
GPT-2-L (Radford et al., 2019)	-	56.5	41.4	68.9	44.6	53.2	52.9
RoBERTa-L (Liu et al., 2019)	-	65.6	45.0	67.6	47.3	57.5	56.6
DeBERTa-v3-L (He et al., 2023)	-	59.9	25.4	44.8	47.8	50.3	45.6
RoBERTa-L (MR; Ma et al., 2021)	AT	70.8	64.2	72.1	63.1	59.6	66.0
Zero-shot Fusion (Kim et al., 2022)	AT, CN, WD, WN	72.5	68.2	72.9	<b>66.6</b>	60.8	68.2
CAR-RoBERTa-L (Wang et al., 2023)	AbsAT	72.7	66.3	73.2	64.0	62.0	67.6
CAR-DeBERTa-v3-L (Wang et al., 2023)	AbsAT	79.6	69.3	78.6	64.0	<u>78.2</u>	73.9
CANDLE-DeBERTa-v3-L (Wang et al., 2024)	CANDLE	<u>81.2</u>	<u>69.9</u>	<u>80.3</u>	65.9	<b>78.3</b>	<u>75.1</u>
CANDLE-VERA-T5-xxl (Wang et al., 2024)	CANDLE	73.8	64.7	77.6	59.4	71.3	69.4
IMAGINE-GPT-2-L	Synthetic VQA	61.5	63.9	68.9	53.0	55.2	58.5
IMAGINE-RoBERTa-L	Synthetic VQA	74.7	67.5	72.3	64.3	61.2	68.0
IMAGINE-DeBERTa-v3-L	Synthetic VQA	<b>82.2</b>	<b>74.0</b>	<b>80.7</b>	<u>66.3</u>	76.7	<b>76.0</b>
Human	-	91.4	88.9	94.9	86.9	94.1	91.2

Table 1: Zero-shot evaluation results on commonsense reasoning tasks (Accuracy %). **Bold** and Underline indicate the best and second-best results, respectively. AT, CN, WD, WN, and AbsAT refer to ATOMIC, ConcretNet, WikiData, WordNet, and AbstractATOMIC. The full comparison is presented in Table 13 (Appendix). The results are from each reference.

Method	$\alpha$ NLI	CSQA	PIQA	SIQA	WG	Avg.
GPT-3.5	61.8	68.9	67.8	<u>68.0</u>	60.7	65.4
ChatGPT	73.2	<b>75.7</b>	<u>81.7</u>	<b>69.7</b>	64.1	<u>72.9</u>
GPT-4	<u>75.0</u>	43.0	73.0	57.0	<b>77.0</b>	65.0
LLaMA2 <sub>13B</sub>	55.9	67.3	80.2	50.3	72.8	65.3
Mistral <sub>7B</sub>	51.0	59.6	<b>83.0</b>	42.9	75.3	62.4
IMAGINE	<b>82.2</b>	<u>74.0</u>	80.7	66.3	<u>76.7</u>	<b>76.0</b>
Human	91.4	88.9	94.9	86.9	94.1	91.2

Table 2: Zero-shot evaluation results of LLMs on commonsense reasoning tasks (Accuracy %). **Bold** and Underline indicate the best and second-best results, respectively. Results are taken from Wang et al. (2024), and IMAGINE represents the results on DeBERTa-v3-L.

Method	QASC	SciQ	ARC-E	ARC-C
SMLM*	26.6	-	33.4	28.4
CAR-RoBERTa-L	56.7	60.7	57.0	36.5
CAR-DeBERTa-v3-L	<u>70.0</u>	<u>76.9</u>	75.3	53.2
OPT <sub>30B</sub> *	39.7	<u>72.7</u>	58.2	34.8
FLAN <sub>137B</sub> *	-	-	<b>79.5</b>	<b>61.7</b>
Z-LaVI (RoBERTa-L)*	27.2	51.3	51.8	33.4
Z-LaVI (BART-L)*	27.3	51.0	56.1	36.5
Z-LaVI (OPT <sub>30B</sub> )*	42.1	74.0	59.5	34.1
IMAGINE-GPT-2-L	<b>46.5</b>	<b>58.4</b>	<u>55.1</u>	35.1
IMAGINE-RoBERTa-L	57.1	63.7	57.9	39.1
IMAGINE-DeBERTa-v3-L	<b>72.4</b>	<b>78.9</b>	<u>76.0</u>	<u>56.2</u>

Table 3: Zero-shot evaluation results on four science question-answering tasks (Accuracy %). **Bold** and Underline indicate the best and second-best results, respectively. Results (\*) are taken from references (Banerjee and Baral, 2020; Yang et al., 2022; Wei et al., 2022)

**Baselines.** We mainly compare IMAGINE with the following zero-shot commonsense reasoning frameworks: MR (Ma et al., 2021), SMLM (Baner-

jee and Baral, 2020), Zero-shot Fusion (Kim et al., 2022), CAR (Wang et al., 2023), and the state-of-the-art framework, CANDLE (Wang et al., 2024). To confirm the efficacy of training with machine imagination in IMAGINE, we also compare it with Z-LaVI (Yang et al., 2022), which leverages machine imagination but does not include the training process. Beyond the reasoning framework based on KBs, we evaluate the recent LLMs, which include LLaMA2<sub>13B</sub> (Touvron et al., 2023), Mistral<sub>7B</sub> (v0.1) (Jiang et al., 2023), OPT<sub>30B</sub> (Zhang et al., 2022), FLAN<sub>137B</sub> (Wei et al., 2022), and the GPT families (i.e., GPT-3.5, ChatGPT (gpt-3.5-turbo), GPT-4).

**Backbones.** To verify the general applicability of IMAGINE, we apply our method to the both encoder and decoder models. Specifically, following the previous works, we utilize RoBERTa-Large (Liu et al., 2019) and DeBERTa-v3-Large (He et al., 2023). Each model has 362M and 443M parameters, respectively. As for the decoder model, we use GPT-2-Large that involves 792M parameters. Implementation details are in Appendix B.

## 4.2 Main Results

Tables 1, 2, and 3 show the results for the commonsense reasoning tasks and the science question-answering tasks. Models based on IMAGINE reveal either superior or competitive performance on overall reasoning tasks. This demonstrates the effectiveness of IMAGINE and highlights the benefit of leveraging machine imagination for reasoning.

In particular, compared to zero-shot common-

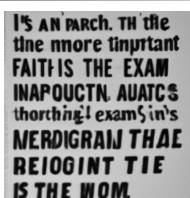
	[PIQA] Q: Brush dust off eyebrows A1: Use toothbrush to groom A2: Use dental floss to groom		[aNLI] Q: Everyone laughed at the funny video. A1. They took a study break to film videos A2. Beth found a funny cat video.
	[CSQA] Q: What part of a table would you put a ruler in? A1. Drawer A2. Desk A3. The backside A4. Office A5. Measure distance		[SIQA] Q: After starting the bar fight Kai told Riley that he had better go quickly. How would you describe Riley? A1. A trouble maker A2. Full of adrenaline A3. A peace maker
	[CSQA] Q: Where usually lacks an elevator but sometimes has a telephone book? A1. At hotel A2. Kitchen A3. Library A4. Telephone booth A5. House		[WG] Q: It is an article of faith that the paper is more important than the exam, even though the _ weighs less heavily on the grade. A1. Paper A2. Exam

Figure 4: Comparison of model predictions and the correctness from IMAGINE and the existing model (Wang et al., 2023) on five commonsense reasoning tasks.

398 sense reasoning frameworks in commonsense reasoning tasks (Table 1), IMAGINE-DeBERTa-v3-L  
399 model surpasses the previous state-of-the-art by  
400 0.9%<sup>p</sup> on average, and specifically by 4.1%<sup>p</sup> on  
401 the CSQA. This suggests that synthetic VQA sig-  
402 nificantly enhances generalization performance in  
403 zero-shot commonsense reasoning. Comparison re-  
404 sults with LLMs (Table 2) also shows that IMAG-  
405 INE outperforms recent LLMs, including ChatGPT  
406 and GPT-4 (OpenAI, 2023). This result suggests  
407 the superior efficiency and effectiveness of IMAG-  
408 INE’s multimodal approach.

409  
410 IMAGINE also proves effective for science QA  
411 tasks (Table 3). Compared to the models with KBs  
412 and larger models, IMAGINE presents better or  
413 competitive reasoning performance. These results  
414 confirm the effectiveness of the machine imagina-  
415 tion capabilities on science-related contexts. We  
416 also highlight the comparison results with Z-LaVI  
417 (Yang et al., 2022) that leverages imagination simi-  
418 lar to ours. IMAGINE outperforms this method by  
419 a significant margin (18.5%<sup>p</sup> on average), under-  
420 scoring the importance of the pre-training phase in  
421 effectively utilizing machine imagination.

### 4.3 Impact of Imagination on Model Inference

422 We analyze the inference results from the text-  
423 based model, CAR (Wang et al., 2023), and IMAG-  
424 INE to confirm the impact of machine imagination  
425 on the model inference. The results are shown in

KB	$\alpha$ NLI	CSQA	PIQA	SIQA	WQ	Avg.
Synthetic VQA	74.7	67.5	72.3	64.3	<b>61.2</b>	<b>68.0</b>
w/o VCR	71.7	65.7	<b>72.3</b>	<b>65.7</b>	60.3	67.1
w/o AbsAT	<b>75.6</b>	<b>67.5</b>	71.7	56.2	58.8	66.0
w/o VCR, AbsAT	65.6	45.0	67.6	47.3	57.5	56.6

Table 4: Ablation results on Synthetic VQA. **Bold** and underline indicate the best and second-best results.

427  
428 Figure 4. We draw three major findings regard-  
429 ing the impact of imagination: (i) When the text  
430 contains limited commonsense knowledge, imagi-  
431 nation indeed helps the model to correctly infer  
432 the answer (First row in the Figure), i.e., positive  
433 impact on predictions (ii) When the generated im-  
434 ages only partially capture the context of the text  
435 query, imagination does not affect the inference re-  
436 sults (Second row in the Figure). (iii) When images  
437 deviate from the real world, imagination can lead  
438 to incorrect inferences (Third row in the Figure).  
439 Specifically, we empirically observe that longer  
440 text queries often result in such cases. These results  
441 suggest that incorporating a text-to-image model  
442 with better alignment capabilities could potentially  
443 mitigate the negative impacts of imagination<sup>4</sup>.

### 4.4 Contributions of Synthetic VQA

444 To confirm the effectiveness of each component  
445 in Synthetic VQA, we evaluate the contribution of

<sup>4</sup>We provide more examples with the visualization of model attention in Appendix F.

LM	ITM	$\alpha$ NLI	CSQA	PIQA	SIQA	WG	Avg.
✓	✓	<b>74.7</b>	<b>67.5</b>	<b>72.3</b>	<b>64.3</b>	<b>61.2</b>	<b>68.0</b>
✓	-	74.3	65.2	71.9	62.3	60.5	66.8
-	✓	71.7	62.0	68.8	60.0	59.6	64.4
-	-	65.6	45.0	67.6	47.3	57.5	56.6

Table 5: Ablation results on pre-training objective of IMAGINE. We use a RoBERTa-L as a backbone.

Inference	$\alpha$ NLI	CSQA	PIQA	SIQA	WG	Avg.
Ensemble	<b>74.7</b>	<b>67.5</b>	<b>72.3</b>	<b>64.3</b>	<b>61.2</b>	<b>68.0</b>
LM	74.1	66.9	71.8	63.8	61.1	67.1
ITM	71.7	63.1	68.3	59.8	59.4	64.0

Table 6: Results of the different inference strategy (LM, ITM). These strategies are evaluated on RoBERTa-L.

AbsAT and VCR. Table 4 presents the results on commonsense reasoning tasks. The model trained only with AbsAT (i.e., w/o VCR) shows superior performance on datasets that contain longer sequences and require complex knowledge (e.g., PIQA, SIQA). In contrast, the model trained only with VCR (i.e., w/o AbsAT) shows its strength on the dataset that contain simpler questions ( $\alpha$ NLI, CSQA) which allows the better use of visual information. When combining these two components, the synthetic VQA results in well-generalized reasoners across diverse reasoning tasks, demonstrating the complementary effect of each component.

#### 4.5 Component Analysis on IMAGINE

**Ablation on Training Objectives.** IMAGINE employs two objectives (i.e., LM, ITM) to learn commonsense knowledge from different modalities. We perform ablations on these objectives to verify their contributions in enhancing zero-shot reasoning capabilities. Table 5 shows the ablation results. Notably, omitting the LM objective leads to a significant drop in performance, underscoring the crucial role of language understanding in commonsense reasoning. Furthermore, while ITM alone does not significantly impact reasoning effectiveness, combining ITM with LM results in improved reasoning performance. These findings suggest that integrating visual information in model optimization leads to better reasoning in commonsense situations.

**Effect of Ensemble Inference.** IMAGINE performs reasoning based on ensemble of the LM and ITM scores. To investigate the contributions in scores obtained from these two different modalities, we evaluate each score independently. The results are presented in Table 6. We observe the lowest

Model	$\alpha$ NLI	CSQA	PIQA	SIQA	WG	Avg.
Adapter	<b>74.7</b>	<b>67.5</b>	<b>72.3</b>	<b>64.3</b>	<b>61.2</b>	<b>68.0</b>
Full	73.0	65.4	71.1	61.5	61.2	66.4

Table 7: Evaluation results of IMAGINE with full fine-tuning (Full) and adapter tuning (Adapter).

performance when evaluating only the ITM scores. However, ensembling LM scores with the ITM results in significant performance improvement across all tasks, even though the scores derived from images are much lower than those from text. This indicates that integrating machine-generated images can complement and enhance language-based reasoning abilities<sup>5</sup>.

**Impact of Adapter.** IMAGINE utilizes adapters (He et al., 2022a) to alleviate the conflicts between the two objectives (i.e., LM, ITM) during the pre-training. In this study, we examine whether separating parameters through adapters for distinct modality objectives is truly effective. Table 7 presents the ablation results on adapters. We observe a significant decline in reasoning performance when adapters are removed. This suggests that direct training of PLMs with images adversely affects the acquisition of textual knowledge. One plausible explanation for this phenomenon is possibly related to catastrophic forgetting (Kirkpatrick et al., 2017), where the model loses previously acquired knowledge (i.e., textual knowledge inherent in PLMs). This highlights the effectiveness of adapters in maintaining the model’s linguistic understanding when it learns from new modalities.

## 5 Conclusion

In this paper, we have proposed IMAGINE, a novel zero-shot commonsense reasoning framework that leverages visual signals to mitigate reporting bias. To steer IMAGINE in effectively utilizing visual information, we have created a large-scale synthetic VQA dataset and optimized the model to jointly use both textual and visual information. We have conducted extensive experiments across a broad range of reasoning tasks. Comprehensive results have shown that IMAGINE establishes new state-of-the-art results on zero-shot commonsense reasoning tasks compared to strong baselines, demonstrating the efficacy of machine imagination.

<sup>5</sup>More analysis on ensemble methods are in Appendix D.

## 521 Limitations

522 We have demonstrated the efficacy of the machine  
523 imagination to improve zero-shot commonsense  
524 reasoning ability. However, we still have the fol-  
525 lowing limitations:

526 **Additional Computations** While machine im-  
527 agination leads to performance improvement in  
528 PLMs, it necessitates additional computations for  
529 generating and processing visual signals. This limi-  
530 tation can be addressed by retrieving relevant im-  
531 ages instead of synthesizing new ones, as demon-  
532 strated in previous work (Yang et al., 2022). We  
533 consider this approach a promising avenue for fu-  
534 ture research.

535 **Exploration of IMAGINE on LLMs** In this work,  
536 we apply IMAGINE to only intermediate-size mod-  
537 els (300M to 790M), as one of our objectives is to  
538 show the smaller models with machine imagination  
539 outperforms LLMs on a broad range of common-  
540 sense reasoning tasks. However, we believe that  
541 IMAGINE can be effectively combined with LLMs,  
542 given that the reporting bias is an inherent issue in  
543 the pre-training corpus and not the models them-  
544 selves. We plan to explore the scaling of machine  
545 imagination in our future research.

## 546 References

547 Pratyay Banerjee and Chitta Baral. 2020. **Self-**  
548 **supervised knowledge triplet learning for zero-shot**  
549 **question answering.** In *Proceedings of the 2020 Con-*  
550 *ference on Empirical Methods in Natural Language*  
551 *Processing.*

552 James Betker, Gabriel Goh, Li Jing, Tim Brooks, Jian-  
553 feng Wang, Linjie Li, Long Ouyang, Juntang Zhuang,  
554 Joyce Lee, Yufei Guo, et al. 2023. Improving image  
555 generation with better captions. *Computer Science.*  
556 <https://cdn.openai.com/papers/dall-e-3.pdf>, 2(3):8.

557 Chandra Bhagavatula, Ronan Le Bras, Chaitanya  
558 Malaviya, Keisuke Sakaguchi, Ari Holtzman, Han-  
559 nah Rashkin, Doug Downey, Wen-tau Yih, and Yejin  
560 Choi. 2020. **Abductive commonsense reasoning.** In  
561 *8th International Conference on Learning Repre-*  
562 *sentations.*

563 Yonatan Bisk, Rowan Zellers, Ronan Le Bras, Jianfeng  
564 Gao, and Yejin Choi. 2020. **PIQA: reasoning about**  
565 **physical commonsense in natural language.** In *The*  
566 *Thirty-Fourth AAAI Conference on Artificial Intelli-*  
567 *gence, The Thirty-Second Innovative Applications of*  
568 *Artificial Intelligence Conference, The Tenth AAAI*  
569 *Symposium on Educational Advances in Artificial*  
570 *Intelligence.*

Antoine Bosselut, Ronan Le Bras, and Yejin Choi. 2021. <b>Dynamic neuro-symbolic knowledge graph construction for zero-shot commonsense question answering.</b> In <i>Thirty-Fifth AAAI Conference on Artificial Intelligence, Thirty-Third Conference on Innovative Applications of Artificial Intelligence, The Eleventh Symposium on Educational Advances in Artificial Intelligence.</i>	571
	572
	573
	574
	575
	576
	577
	578
Tom B. Brown, Benjamin Mann, Nick Ryder, Melanie Subbiah, Jared Kaplan, Prafulla Dhariwal, Arvind Neelakantan, Pranav Shyam, Girish Sastry, Amanda Askell, Sandhini Agarwal, Ariel Herbert-Voss, Gretchen Krueger, Tom Henighan, Rewon Child, Aditya Ramesh, Daniel M. Ziegler, Jeffrey Wu, Clemens Winter, Christopher Hesse, Mark Chen, Eric Sigler, Mateusz Litwin, Scott Gray, Benjamin Chess, Jack Clark, Christopher Berner, Sam McCandlish, Alec Radford, Ilya Sutskever, and Dario Amodei. 2020. <b>Language models are few-shot learners.</b> In <i>Advances in Neural Information Processing Systems 33: Annual Conference on Neural Information Processing Systems 2020.</i>	579
	580
	581
	582
	583
	584
	585
	586
	587
	588
	589
	590
	591
	592
Peter Clark, Isaac Cowhey, Oren Etzioni, Tushar Khot, Ashish Sabharwal, Carissa Schoenick, and Oyvind Tafjord. 2018. <b>Think you have solved question answering? try arc, the AI2 reasoning challenge.</b> <i>CoRR</i> , abs/1803.05457.	593
	594
	595
	596
	597
Wenliang Dai, Junnan Li, Dongxu Li, Anthony Meng Huat Tiong, Junqi Zhao, Weisheng Wang, Boyang Li, Pascale Fung, and Steven C. H. Hoi. 2023. <b>Instructclip: Towards general-purpose vision-language models with instruction tuning.</b> In <i>Advances in Neural Information Processing Systems 36: Annual Conference on Neural Information Processing Systems 2023.</i>	598
	599
	600
	601
	602
	603
	604
	605
Banchiamlack Dessalegn and Barbara Landau. 2013. <b>Interaction between language and vision: It's momentary, abstract, and it develops.</b> <i>Cognition</i> , 127:331–344.	606
	607
	608
	609
Jacob Devlin, Ming-Wei Chang, Kenton Lee, and Kristina Toutanova. 2019. <b>BERT: pre-training of deep bidirectional transformers for language understanding.</b> In <i>Proceedings of the 2019 Conference of the North American Chapter of the Association for Computational Linguistics: Human Language Technologies.</i>	610
	611
	612
	613
	614
	615
	616
Zi-Yi Dou and Nanyun Peng. 2022. <b>Zero-shot commonsense question answering with cloze translation and consistency optimization.</b> In <i>Thirty-Sixth AAAI Conference on Artificial Intelligence, Thirty-Fourth Conference on Innovative Applications of Artificial Intelligence, The Twelfth Symposium on Educational Advances in Artificial Intelligence.</i>	617
	618
	619
	620
	621
	622
	623
Weixi Feng, Xuehai He, Tsu-Jui Fu, Varun Jampani, Arjun R. Akula, Pradyumna Narayana, Sugato Basu, Xin Eric Wang, and William Yang Wang. 2023. <b>Training-free structured diffusion guidance for compositional text-to-image synthesis.</b> In <i>The Eleventh</i>	624
	625
	626
	627
	628

629	<i>International Conference on Learning Representations.</i>	James Kirkpatrick, Razvan Pascanu, Neil Rabinowitz, Joel Veness, Guillaume Desjardins, Andrei A Rusu, Kieran Milan, John Quan, Tiago Ramalho, Agnieszka Grabska-Barwinska, et al. 2017. Overcoming cata- strophic forgetting in neural networks. <i>Proceedings of the national academy of sciences</i> , 114(13):3521– 3526.	684
630			685
631	Linda B. Gambrell and Ruby J. Bales. 1986. Mental imager and the comprehension-monitoring perfor- mance of fourth- and fifth-grade poor readers. <i>Read- ing Research Quarterly</i> , 21:454.		686
632			687
633			688
634			689
635	Jonathan Gordon and Benjamin Van Durme. 2013. Re- porting bias and knowledge acquisition. In <i>Pro- ceedings of the 2013 workshop on Automated knowl- edge base construction</i> .		690
636			
637			
638			
639	Xin Guan, Biwei Cao, Qingqing Gao, Zheng Yin, Bo Liu, and Jiuxin Cao. 2023. Multi-hop com- monsense knowledge injection framework for zero- shot commonsense question answering. <i>CoRR</i> , abs/2305.05936.	Junnan Li, Dongxu Li, Silvio Savarese, and Steven C. H. Hoi. 2023. BLIP-2: bootstrapping language-image pre-training with frozen image encoders and large language models. In <i>Proceedings of the 40th Inter- national Conference on Machine Learning</i> , volume 202, pages 19730–19742.	691
640			692
641			693
642			694
643			695
644	David Gunning. 2018. Machine common sense concept paper. <i>arXiv preprint arXiv:1810.07528</i> .	Xiang Lorraine Li, Adhiguna Kuncoro, Jordan Hoff- mann, Cyprien de Masson d’Autume, Phil Blunsom, and Aida Nematzadeh. 2022. A systematic investiga- tion of commonsense knowledge in large language models. In <i>Proceedings of the 2022 Conference on Empirical Methods in Natural Language Processing</i> .	696
645			700
646			701
647			702
648			
649			
650			
651	Junxian He, Chunting Zhou, Xuezhe Ma, Taylor Berg- Kirkpatrick, and Graham Neubig. 2022a. Towards a unified view of parameter-efficient transfer learning. In <i>The Tenth International Conference on Learning Representations</i> .	Jiacheng Liu, Wenya Wang, Dianzhuo Wang, Noah A. Smith, Yejin Choi, and Hannaneh Hajishirzi. 2023. Vera: A general-purpose plausibility estimation model for commonsense statements. In <i>Proceed- ings of the 2023 Conference on Empirical Methods in Natural Language Processing</i> .	703
652			704
653			705
654			706
655	Mutian He, Tianqiang Fang, Weiqi Wang, and Yangqiu Song. 2022b. Acquiring and modelling abstract com- monsense knowledge via conceptualization. <i>CoRR</i> , abs/2206.01532.	Xiao Liu, Da Yin, Yansong Feng, and Dongyan Zhao. 2022. Things not written in text: Exploring spatial commonsense from visual signals. In <i>Proceedings of the 60th Annual Meeting of the Association for Computational Linguistics</i> .	709
656			710
657			711
658			712
659			713
660	Pengcheng He, Jianfeng Gao, and Weizhu Chen. 2023. Debertav3: Improving deberta using electra-style pre- training with gradient-disentangled embedding shar- ing. In <i>The Eleventh International Conference on Learning Representations</i> .	Yinhan Liu, Myle Ott, Naman Goyal, Jingfei Du, Man- dar Joshi, Danqi Chen, Omer Levy, Mike Lewis, Luke Zettlemoyer, and Veselin Stoyanov. 2019. Roberta: A robustly optimized BERT pretraining ap- proach. <i>CoRR</i> , abs/1907.11692.	714
661			715
662			716
663			717
664			718
665			
666			
667	Albert Q. Jiang, Alexandre Sablayrolles, Arthur Men- sch, Chris Bamford, Devendra Singh Chaplot, Diego de Las Casas, Florian Bressand, Gianna Lengyel, Guillaume Lample, Lucile Saulnier, Lélio Ren- nard Lavaud, Marie-Anne Lachaux, Pierre Stock, Teven Le Scao, Thibaut Lavril, Thomas Wang, Timo- thèque Lacroix, and William El Sayed. 2023. Mistral 7b. <i>CoRR</i> , abs/2310.06825.	Yujie Lu, Wanrong Zhu, Xin Wang, Miguel Eck- stein, and William Yang Wang. 2022. Imagination- augmented natural language understanding. In <i>Pro- ceedings of the 2022 Conference of the North Amer- ican Chapter of the Association for Computational Linguistics: Human Language Technologies</i> .	719
668			720
669			721
670			722
671			723
672			724
673			
674			
675			
676	Tushar Khot, Peter Clark, Michal Guerquin, Peter Jansen, and Ashish Sabharwal. 2020. QASC: A dataset for question answering via sentence composi- tion. In <i>The Thirty-Fourth AAAI Conference on Arti- ficial Intelligence, The Thirty-Second Innovative Ap- plications of Artificial Intelligence Conference, The Tenth AAAI Symposium on Educational Advances in Artificial Intelligence</i> .	Kaixin Ma, Filip Ilievski, Jonathan Francis, Yonatan Bisk, Eric Nyberg, and Alessandro Oltramari. 2021. Knowledge-driven data construction for zero-shot evaluation in commonsense question answering. In <i>Thirty-Fifth AAAI Conference on Artificial Intelli- gence</i> .	725
677			726
678			727
679			728
680			729
681			730
682			
683	Yu Jin Kim, Beong-woo Kwak, Youngwook Kim, Reinald Kim Amplayo, Seung-won Hwang, and Jiny- oung Yeo. 2022. Modularized transfer learning with multiple knowledge graphs for zero-shot common- sense reasoning. In <i>Proceedings of the 2022 Con- ference of the North American Chapter of the Asso- ciation for Computational Linguistics: Human Lan- guage Technologies</i> .	Arindam Mitra, Pratyay Banerjee, Kuntal Kumar Pal, Swaroop Mishra, and Chitta Baral. 2019. Exploring ways to incorporate additional knowledge to improve natural language commonsense question answering. <i>CoRR</i> , abs/1909.08855.	731
684			732
685			733
686			734
687			735
688			
689			
690			
691			
692			
693			
694			
695			
696			
697			
698			
699			
700			
701			
702			
703			
704			
705			
706			
707			
708			
709			
710			
711			
712			
713			
714			
715			
716			
717			
718			
719			
720			
721			
722			
723			
724			
725			
726			
727			
728			
729			
730			
731			
732			
733			
734			
735			

738	Alec Radford, Jong Wook Kim, Chris Hallacy, Aditya Ramesh, Gabriel Goh, Sandhini Agarwal, Girish Sastry, Amanda Askell, Pamela Mishkin, Jack Clark, Gretchen Krueger, and Ilya Sutskever. 2021. Learning transferable visual models from natural language supervision. In <i>Proceedings of the 38th International Conference on Machine Learning</i> , volume 139 of <i>Proceedings of Machine Learning Research</i> .	795
739		796
740		797
741		798
742		
743		
744		
745		
746	Alec Radford, Jeffrey Wu, Rewon Child, David Luan, Dario Amodei, Ilya Sutskever, et al. 2019. Language models are unsupervised multitask learners. <i>OpenAI blog</i> , 1(8):9.	799
747		800
748		801
749		802
750		803
751		804
752		805
753		
754		
755	Robin Rombach, Andreas Blattmann, Dominik Lorenz, Patrick Esser, and Björn Ommer. 2022. High-resolution image synthesis with latent diffusion models. In <i>IEEE/CVF Conference on Computer Vision and Pattern Recognition</i> .	806
756		807
757		808
758		809
759		810
760		
761		
762		
763	Keisuke Sakaguchi, Ronan Le Bras, Chandra Bhagavatula, and Yejin Choi. 2020. Winogrande: An adversarial winograd schema challenge at scale. In <i>The Thirty-Fourth AAAI Conference on Artificial Intelligence, The Thirty-Second Innovative Applications of Artificial Intelligence Conference, The Tenth AAAI Symposium on Educational Advances in Artificial Intelligence</i> .	811
764		812
765		813
766		814
767		815
768		816
769		817
770		818
771		819
772	Maarten Sap, Ronan Le Bras, Emily Allaway, Chandra Bhagavatula, Nicholas Lourie, Hannah Rashkin, Brendan Roof, Noah A. Smith, and Yejin Choi. 2019a. ATOMIC: an atlas of machine commonsense for if-then reasoning. In <i>The Thirty-Third AAAI Conference on Artificial Intelligence, The Thirty-First Innovative Applications of Artificial Intelligence Conference, The Ninth AAAI Symposium on Educational Advances in Artificial Intelligence</i> .	820
773		821
774		822
775		823
776		824
777		825
778		826
779		827
780		828
781		829
782		830
783		831
784	Maarten Sap, Hannah Rashkin, Derek Chen, Ronan Le Bras, and Yejin Choi. 2019b. Social iqa: Commonsense reasoning about social interactions. In <i>Proceedings of the 2019 Conference on Empirical Methods in Natural Language Processing and the 9th International Joint Conference on Natural Language Processing</i> .	832
785		833
786		
787		
788		
789	Vered Shwartz, Peter West, Ronan Le Bras, Chandra Bhagavatula, and Yejin Choi. 2020. Unsupervised commonsense question answering with self-talk. In <i>Proceedings of the 2020 Conference on Empirical Methods in Natural Language Processing</i> .	834
790		835
791		
792		
793	Yangqiu Song, Haixun Wang, Zhongyuan Wang, Hongsong Li, and Weizhu Chen. 2011. Short text conceptualization using a probabilistic knowledgebase. In <i>Proceedings of the 22nd International Joint Conference on Artificial Intelligence</i> .	836
794		837
795		838
796		839
797		840
798		841
799	Weiwei Wang, Tianqing Fang, Wenxuan Ding, Baixuan Xu, Xin Liu, Yangqiu Song, and Antoine Bosselut. 2023. CAR: conceptualization-augmented reasoner for zero-shot commonsense question answering. In <i>Findings of the Association for Computational Linguistics: EMNLP 2023</i> .	842
800		843
801		844
802		845
803		846
804		847
805		848
806	Weiwei Wang, Tianqing Fang, Chunyang Li, Haochen Shi, Wenxuan Ding, Baixuan Xu, Zhaowei Wang, Jiaxin Bai, Xin Liu, Jiayang Cheng, Chunkit Chan, and Yangqiu Song. 2024. CANDLE: iterative conceptualization and instantiation distillation from large language models for commonsense reasoning. <i>CoRR</i> , abs/2401.07286.	849
807		850
808		851
809		852
810		
811	Jason Wei, Maarten Bosma, Vincent Y. Zhao, Kelvin Guu, Adams Wei Yu, Brian Lester, Nan Du, Andrew M. Dai, and Quoc V. Le. 2022. Finetuned language models are zero-shot learners. In <i>The Tenth</i>	849
812		850
813		851
814		852

853        *International Conference on Learning Representations.*  
854

855        Johannes Welbl, Nelson F. Liu, and Matt Gardner. 2017.  
856        **Crowdsourcing multiple choice science questions.**  
857        In *Proceedings of the 3rd Workshop on Noisy User-*  
858        *generated Text.*

859        Yue Yang, Wenlin Yao, Hongming Zhang, Xiaoyang  
860        Wang, Dong Yu, and Jianshu Chen. 2022. **Z-lavi:**  
861        **Zero-shot language solver fueled by visual imagi-**  
862        **nation.** In *Proceedings of the 2022 Conference on*  
863        *Empirical Methods in Natural Language Processing.*

864        Rowan Zellers, Yonatan Bisk, Ali Farhadi, and Yejin  
865        Choi. 2019. **From recognition to cognition: Visual**  
866        **commonsense reasoning.** In *IEEE Conference on*  
867        *Computer Vision and Pattern Recognition.*

868        Susan Zhang, Stephen Roller, Naman Goyal, Mikel  
869        Artetxe, Moya Chen, Shuhui Chen, Christopher  
870        Dewan, Mona T. Diab, Xian Li, Xi Victoria Lin,  
871        Todor Mihaylov, Myle Ott, Sam Shleifer, Kurt Shus-  
872        ter, Daniel Simig, Punit Singh Koura, Anjali Srid-  
873        har, Tianlu Wang, and Luke Zettlemoyer. 2022.  
874        **OPT: open pre-trained transformer language mod-**  
875        **els.** *CoRR*, abs/2205.01068.

876        Deyao Zhu, Jun Chen, Xiaoqian Shen, Xiang Li, and  
877        Mohamed Elhoseiny. 2023. **Minigpt-4: Enhancing**  
878        **vision-language understanding with advanced large**  
879        **language models.** *CoRR*, abs/2304.10592.

## Appendix

### A Synthetic VQA dataset

	Train	Dev	Total
# Images generated from AbsAT	18,838	1,695	20,533
# QA pairs from AbsAT	486,778	46,238	533,016
# Images from VCR	80,418	9,929	90,347
# QA pairs from VCR	212,923	26,534	239,457
# Total Images	99,256	11,624	110,880
# Total QA pairs	699,701	72,772	772,473

Table 8: Statistic of synthetic VQA dataset.

We construct a synthetic VQA dataset using AbstractATOMIC and VCR. First, we generate images using the questions from AbstractATOMIC. Since AbstractATOMIC consists only of text, we need to create images based on these questions. In this process, we standardize all the person names in the questions to “Person” and remove duplicate questions, resulting in approximately 20K images. To include more realistic images and common-sense questions corresponding to those images, we extract question-answer pairs from VCR images. However, most of these questions are directly related to the images, making it difficult to answer without them, which poses a challenge for LM-based training. To address this, we replace the person indices in the questions with gender-neutral names and generate captions for the images to use as prefixes for the questions. In addition, each QA pair from VCR has four answer candidates, while each pair from AbstractATOMIC has three candidates. To combine them, we match the number of answer choices by randomly discarding one distractor from VCR. The statistic of our dataset is provided in Table 8.

### B Implementation Details

To construct the VQA pairs, we primarily use DALL-E 3-XL (Betker et al., 2023), a powerful image synthesis model. For generating images in the synthetic VQA dataset, we first remove overly specific information, such as personal names, from the questions. Then, we generate images with a resolution of  $384 \times 384$  using 50 inference steps. During the evaluation, we generate  $512 \times 512$  images for each task based on the questions, maintaining the same number of inference steps. We use the CLIP-Large (Radford et al., 2021) model to extract image features. Following prior work, we use two power-

IMAGINE	GPT-2-L	RoBERTa-L	DeBERTa-v3-L
Image Encoder	CLIP-ViT-L/14		
# Params.	792M + 428M	362M + 428M	443M + 428M
# Trainable Params.	7.9M	8.4M	8.4M
Training Time	70h	30h	80h
Batch Size		8, 16, <b>32</b> , 64	
Learning Rate		7e-6, <b>1e-5</b> , 3e-5	
Epoch			2

Table 9: Detailed training settings for IMAGINE. **Bold** indicates the chosen hyperparameter.

ful PLMs as the backbone. We add Parallel Adapter (He et al., 2022a) with a reduction factor of 16 to each model and freeze all parameters except for the adapters. We follow the training settings of Ma et al. (2021) and Wang et al. (2023) to train Transformer decoder-based and encoder-based model for the in-depth comparison. We report our results derived from the ensemble score using the optimal ensemble weight for each task. All experiments are conducted using four NVIDIA A5000 GPUs. More details are presented in Table 9.

### C Impact of Image Quality

We aim to observe the changes in inference performance based on image quality by generating images of various qualities using three different methods. First, similar to our main experiment, we utilize the questions from the evaluation dataset to generate images with a resolution of  $512 \times 512$  using both DALL-E 3-XL and the Latent Diffusion Model (LDM; Rombach et al., 2022), which has relatively lower image synthesis capabilities. Additionally, we generate images with a resolution of  $384 \times 384$  using DALL-E 3-XL, following the same method used for creating the synthetic VQA dataset.

IMAGINE	$\alpha$ NLI	CSQA	PIQA	SIQA	WG	Avg.
Text only	73.2	66.3	71.3	64.5	60.3	67.1
LDM ( $512 \times 512$ )	73.2	66.3	71.9	64.3	60.6	67.3
DALL-E 3 ( $384 \times 384$ )	74.5	66.8	71.9	64.3	60.6	67.6
DALL-E 3 ( $512 \times 512$ )	<b>74.7</b>	<b>67.5</b>	<b>72.3</b>	<b>64.3</b>	<b>61.2</b>	<b>68.0</b>

Table 10: Results of using various image synthesis models for evaluation. The numbers in parentheses indicate the image resolution.

The results in Table 10 show that the IMAGINE with the LDM model performs the worst, indicating that utilizing a less effective image synthesis model can degrade overall performance. However, all models benefit from incorporating various resolutions of images. As seen in Figure 5, this is likely because the generated images, despite varying in

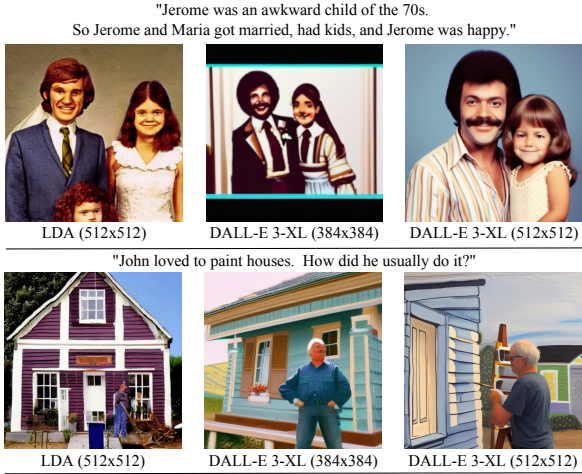


Figure 5: Comparison of generated images. The sentences are the queries used to generate the images.

quality, mostly maintain contextual relevance to the query sentences, thereby having a similar positive impact on the inference results.

## D Ensemble Methods

To verify the effectiveness of our framework’s multimodality approach, we train two unimodal models using different seeds on the synthetic VQA dataset, utilizing only the text. We then ensemble the scores obtained from these two models. The results are presented in Table 11. While ensembling scores from single modalities (LM+LM) provides performance benefits, ensembling scores from two different modalities (LM+ITM), as done in IMAGINE, proves to be the most effective. This demonstrates that the multimodality approach plays a crucial role in enhancing zero-shot reasoning performance.

RoBERTa-Large	$\alpha$ NLI	CSQA	PIQA	SIQA	WG	Avg.
LM	74.3	65.2	71.9	62.3	60.5	66.8
LM+LM	74.3	66.0	72.1	64.2	60.4	67.4
LM+ITM (IMAGINE)	<b>74.7</b>	<b>67.5</b>	<b>72.3</b>	<b>64.3</b>	<b>61.2</b>	<b>68.0</b>

Table 11: Results of two different ensemble methods.

We report the optimal ensemble weights used for our framework in Figure 6. The larger the ensemble weight, the greater the influence of the image scores. Additionally, we draw a line indicating the average accuracy in each plot. From this, we can infer that the DeBERTa-v3-Large model utilizes image information more extensively than the RoBERTa-Large. When applying IMAGINE to DeBERTa-v3-Large, the performance improvement is greater than when using RoBERTa-Large, sug-

gesting that visual information contributes positively to most reasoning tasks.

## E IMAGINE with Decoder-based Model

We conducted experiments using GPT-2, a widely-used decoder-based generative language model, to verify the applicability to recent language models. We follow the settings of (Ma et al., 2021) to train to model on synthetic datasets.

	$\alpha$ NLI	CSQA	PIQA	SIQA	WG	Avg.
GPT-2-L	56.5	41.4	68.9	44.6	53.2	52.9
GPT-2-L (MR)	59.2	48.0	67.5	53.6	54.7	56.6
CAR-GPT-2-L	61.7	50.0	68.2	52.3	55.2	57.5
IMAGINE-GPT-2-L	61.5	53.9	68.9	53.0	55.2	58.5

Table 12: Zero-shot evaluation results with decoder-only generative model.

The results in Table 12 demonstrate that IMAGINE is effective not only for encoder-based models but also for decoder-based models. Based on these findings, we plan to address methodologies in future work that can effectively utilize images while preserving the rich language understanding capabilities of large language models.

## F Visualization of Image Attention

We aim to visualize how the model utilizes specific parts of an image. The formula to compute contextualized visual features used for computing the ITM score calculation process is similar to the attention algorithm, allowing us to derive attention scores for each image patch. Based on these scores, we erase 100 image patches with the lowest scores to understand which parts the model focuses on. As shown in Figure 7, 8, and 9, each model tends to assign relatively high attention scores to objects related to the question in most cases, rather than using the image patches randomly. This is notable because the model can effectively capture the relationship between text and images using adapters, despite training with much less data compared to existing visual-language modeling studies (Li et al., 2023; Zhu et al., 2023). In addition, we observe that the DeBERTa-v3-Large model tends to focus more frequently on the correct parts than the RoBERTa-Large model. Figure 7 shows these cases clearly. This aligns with the result that the IMAGINE is more effective with DeBERTa-v3-Large, suggesting that a model with high generalization performance is also useful for learning new modalities.

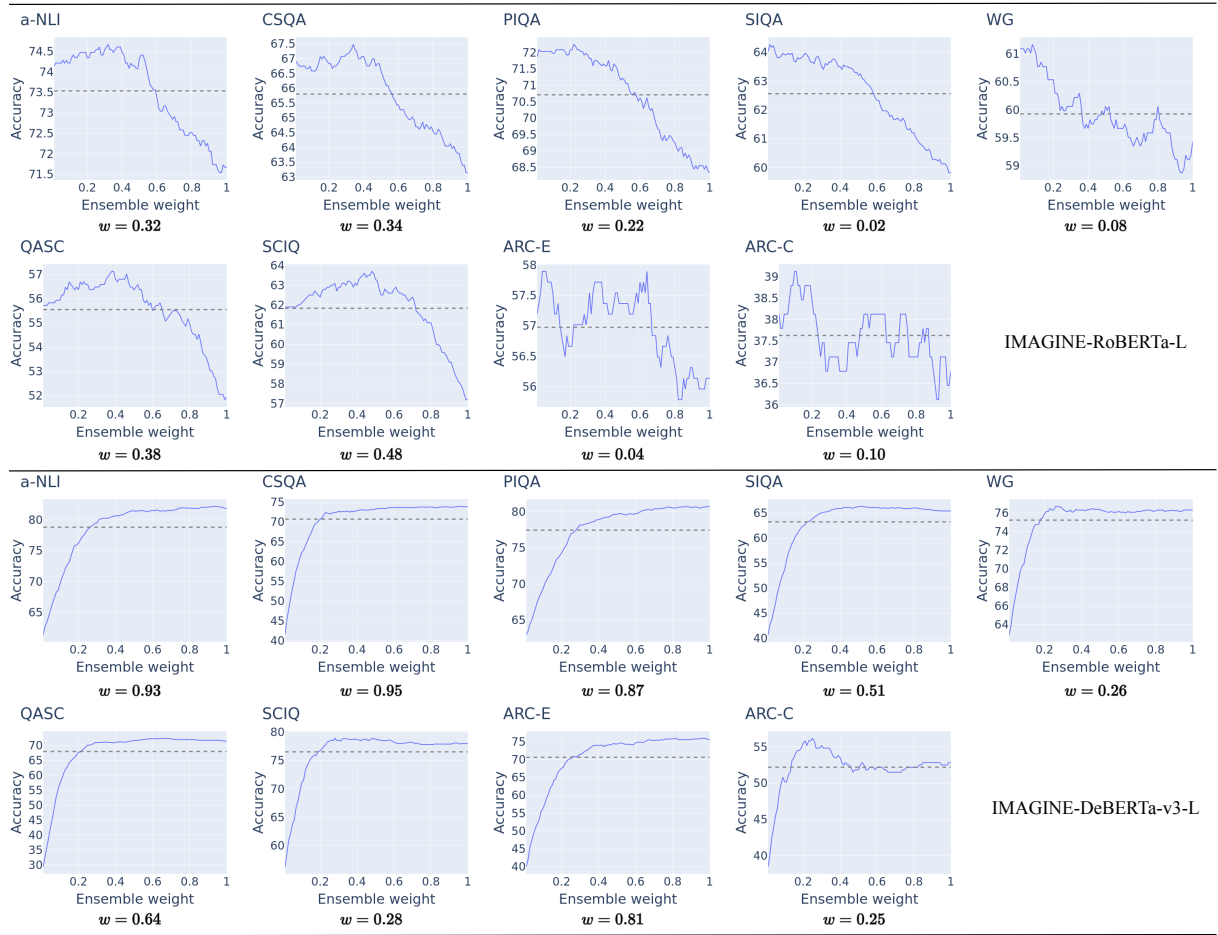


Figure 6: Model accuracy variation with different ensemble weights. The optimal  $w$  for each task is shown below the plots. The line in the middle indicates the average accuracy.

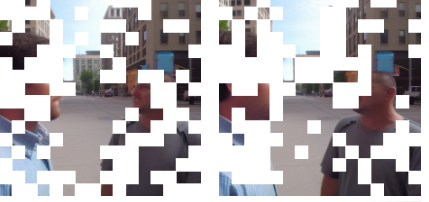
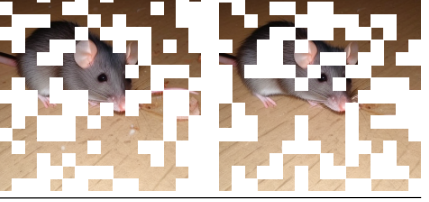
		DeBERTa-v3-L	RoBERTa-L
<p>Q. Joe was walking through downtown. He reluctantly agreed to give them an interview. A1. He was approached by a pretty woman. <b>A2. He was approached by a survey taker.</b></p>	DeBERTa-v3-L: A2 (O)      RoBERTa-L: A1 (X)		
<p>Q. I got up from a nap feeling very hungry. After the inspector arrived and killed the rats, I felt very happy. <b>A1. I decided not to eat when I saw a rat in the kitchen.</b> A2. I ate a lot of rats in my kitchen.</p>	DeBERTa-v3-L: A1 (O)      RoBERTa-L: A1 (O)		
<p>Q. John didn't mind getting in line. It was what game after that he hated. The time, the sore feet. He did not like doing what? A1. Have to wait for   <b>A2. Standing in line</b>    A3. Eat cake A4. Less confusion    A5. Being ordered</p>	DeBERTa-v3-L: A2 (O)      RoBERTa-L: A2 (O)		
<p>Q. Of all the sports, Billy enjoys football, but what does his concerned mother think of the sport? A1. Very entertaining    A2. Fun    A3. Competitive A4. Competitive    <b>A5. Violent</b></p>	DeBERTa-v3-L: A5 (O)      RoBERTa-L: A2 (X)		
<p>Q. How to quickly cool down a bottled water drink? A1. Run the paper towel under some water and wrap a bottle around it then place in the freezer for 20 minutes. <b>A2. Run the bottle under some water and wrap a paper towel around it then place in the freezer for 20 minutes.</b></p>	DeBERTa-v3-L: A2 (O)      RoBERTa-L: A2 (O)		
<p>Q. What is the best way to apply nail polish to a professional result? A1. A quick way to apply nail polish is to use a large brush, then cover any messy areas with flesh-colored nail polish. <b>A2. Tape the cuticles with snugly fitting tape, then paint the nails. Remove the tape and use a nail polish remover-soaked q-tip to clean any excess polish from the cuticles or fingers.</b></p>	DeBERTa-v3-L: A2 (O)      RoBERTa-L: A2 (O)		

Figure 7: Randomly sampled examples from IMAGINE alongside the visualization of image attention from the Abductive NLI, CommonsenseQA, and PIQA validation sets.

		DeBERTa-v3-L	RoBERTa-L
Q.	Robin studied hard the night before, and found the test to be very easy. Robin finished the test quickly. How would Robin feel afterwards?		
A1.	<b>Proud</b>	A2. Motivated	
A3.	Nervous		
	DeBERTa-v3-L: A1 (O)      RoBERTa-L: A1 (O)		
Q.	Alex bought his entire team gold watches and when he gave them the present he put each watch on their wrist himself. How would you describe Alex?		
A1.	A greedy person	A2. Satisfied over the gift he gave his team	
A3.	<b>A thoughtful person</b>		
	DeBERTa-v3-L: A1 (X)      RoBERTa-L: A3 (O)		
Q.	As a parent, Catherine doesn't let her kids watch movies, but they can watch some TV shows. Catherine thinks the _____ are too violent.		
A1.	<b>Movies</b>	A2. TV shows	
	DeBERTa-v3-L: A1 (O)      RoBERTa-L: A1 (O)		
Q.	The farmer had more corn to harvest than yams because his cow hated eating the _____.		
A1.	Yam	A2. Corn	
	DeBERTa-v3-L: A1 (X)      RoBERTa-L: A1 (X)		
Q.	What cycle is the most directly affected by the combustion of fossil fuels?		
A1.	Rock cycle	A2. Water cycle	
A4.	Nitrogen cycle		
	DeBERTa-v3-L: A3 (O)      RoBERTa-L: A3 (O)		
Q.	What energy change takes place when a piece of bread is toasted in a toaster?		
A1.	Chemical energy to light energy	A2. <b>Electrical energy to heat energy</b>	
A3.	Heat energy to chemical energy		
A4.	Light energy to electrical energy		
	DeBERTa-v3-L: A2 (O)      RoBERTa-L: A3 (X)		

Figure 8: Randomly sampled examples from IMAGINE alongside the visualization of image attention from the SIQA, Winogrande, and ARC-easy validation sets.

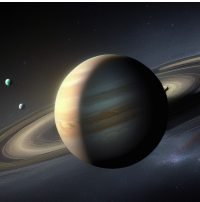
		DeBERTa-v3-L	RoBERTa-L
Q. Where would it be most dangerous to work with electric tools?	A1. In a garage A2. Beside a swimming pool A3. Near a television or computer A4. In a cool basement		
DeBERTa-v3-L: A2 (X)      RoBERTa-L: A2 (X)			
Q. When the motion of liquid water molecules slow, what most likely happens?	A1. The liquid water forms a solid A2. The liquid water condenses A3. The liquid water undergoes a chemical change A4. The liquid water becomes a vapor		
DeBERTa-v3-L: A2 (X)      RoBERTa-L: A3 (X)			
Q. What is changing globally?	A1. The number of countries.      A2. rapid growth A3. How they move      A4. Temperature and moisture A5. Differences in speed      A6. Net biomass A7. Occurs over a wide range      A8. Exposure to oxygen and water		
DeBERTa-v3-L: A4 (O)      RoBERTa-L: A1 (X)			
Q. What has tiny hairs that trap particles?	A1. Sponges      A2. Molecules A3. Oaks      A4. Lizards A5. Protozoa      A6. Snakes A7. Cilia      A8. Clouds		
DeBERTa-v3-L: A7 (X)      RoBERTa-L: A4 (X)			
Q. What are the outer planets of the solar system made of?	A1. Solids      A2. Plasma      A3. Liquids      A4. Gases		
DeBERTa-v3-L: A4 (O)      RoBERTa-L: A4 (O)			
Q. What do we call cyclones that form in tropical latitudes?	A1. Eruptions      A2. Twister      A3. Disturbances      A4. hurricanes		
DeBERTa-v3-L: A4 (O)      RoBERTa-L: A4 (O)			

Figure 9: Randomly sampled examples from IMAGINE alongside the visualization of image attention from the ARC-challenge, QASC, and SciQ validation sets.

Method	KB	$\alpha$ NLI	CSQA	PIQA	SIQA	WG	Avg.
<b>Pre-trained Language Models</b>							
GPT-2-L (Radford et al., 2019)	-	56.5	41.4	68.9	44.6	53.2	52.9
RoBERTa-L (Liu et al., 2019)	-	65.6	45.0	67.6	47.3	57.5	56.6
DeBERTa-v3-L (He et al., 2023)	-	59.9	25.4	44.8	47.8	50.3	45.6
Self-talk (Shwartz et al., 2020)	-	-	32.4	70.2	46.2	54.7	-
COMET-DynGen (Bosselut et al., 2021)	AT	-	-	-	50.1	-	-
SMLM (Banerjee and Baral, 2020)	*	65.3	38.8	-	48.5	*	-
GPT-2-L (MR; Ma et al., 2021)	AT	59.2	48.0	67.5	53.6	54.7	56.6
RoBERTa-L (MR; Ma et al., 2021)	AT	70.8	64.2	72.1	63.1	59.6	66.0
DeBERTa-v3-L (MR; Ma et al., 2021)	AT	76.0	67.0	78.0	62.1	76.0	71.8
MICO (Su et al., 2022)	AT	-	44.2	-	56.0	-	-
Zero-shot Fusion (Kim et al., 2022)	AT, CN, WD, WN	72.5	68.2	72.9	66.6	60.8	68.2
Multi-hop Knowledge Injection (Guan et al., 2023)	AT, CN, WD, WN	72.5	71.0	73.1	-	61.0	-
CAR-GPT-2-L (Wang et al., 2023)	AbsAT	61.7	50.0	68.2	52.3	55.2	57.5
CAR-RoBERTa-L (Wang et al., 2023)	AbsAT	72.7	66.3	73.2	64.0	62.0	67.6
CAR-DeBERTa-v3-L (Wang et al., 2023)	AbsAT	79.6	69.3	78.6	64.0	<u>78.2</u>	73.9
CANDLE-DeBERTa-v3-L (Wang et al., 2024)	CANDLE	81.2	69.9	80.3	65.9	<b>78.3</b>	75.1
<b>Large Language Models</b>							
GPT-3.5 (text-davinci-003)	-	61.8	68.9	67.8	68.0	60.7	65.4
ChatGPT (gpt-3.5-turbo)	-	73.2	<b>75.7</b>	81.7	<b>69.7</b>	64.1	72.9
GPT-4 (gpt-4)	-	75.0	43.0	73.0	57.0	77.0	65.0
LLAMA2-13B (Touvron et al., 2023)	-	55.9	67.3	80.2	50.3	72.8	65.3
Mistral-v0.1-7B (Jiang et al., 2023)	-	51.0	59.6	<b>83.0</b>	42.9	75.3	62.4
VERA-T5-xxl (Liu et al., 2023)	AT	71.2	61.7	76.4	58.2	67.2	66.9
VERA-T5-xxl (Liu et al., 2023)	AbsAT	73.2	63.0	77.2	58.1	68.1	68.0
CANDLE-VERA-T5-xxl (Wang et al., 2024)	CANDLE	73.8	64.7	77.6	59.4	71.3	69.4
<b>Ours</b>							
IMAGINE-GPT-2-L	Synthetic VQA	61.5	63.9	68.9	53.0	55.2	58.5
IMAGINE-RoBERTa-L	Synthetic VQA	74.7	67.5	72.3	64.3	61.2	68.0
IMAGINE-DeBERTa-v3-L	Synthetic VQA	<b>82.2</b>	74.0	80.7	66.3	76.7	<b>76.0</b>
<b>Supervised &amp; Human</b>							
RoBERTa-L (Supervised)	-	85.6	78.5	79.2	76.6	79.3	79.8
DeBERTa-v3-L (Supervised)	-	89.0	82.1	84.5	80.1	84.1	84.0
Human	-	91.4	88.9	94.9	86.9	94.1	91.2

Table 13: Zero-shot evaluation results on five commonsense reasoning tasks (Accuracy %). **Bold** and Underline indicate the best and second-best results, respectively. AT, CN, WD, WN, and AbsAT refer to ATOMIC, ConceptNet, WikiData, WordNet, and AbstractATOMIC. The results of the large language models including GPT series are taken from Wang et al. (2024). SMLM (\*) used different KBs for the different benchmarks.